ISSN No:-2456-2165 https://doi.org/10.38124/ijisrt/26jul999

Evaluating the Contraceptive Efficacy and Hormonal Profiles of *Ricinus communis* Linn, Clomiphene Citrate and Exogenous Estrogen

F. Shinku[1*]; M. A. Wazhi[2]; V. E. Odey[3]; P. Nyango[4]; M. B. Mohammed[5]; C. N. Edeh[6]; N. Z. Nden[7]; S. S. Gotom[8]; J. S. Kumbet[9]; S. A. Adamu[10]; N. J. Chuwang[11]; Y. M. Usman[12]; M. O. Omolara[13]; R. J. Kutshik[14]; R.T. Mcneil[15]

[1,2,3,4,5,6,7,11&12]Department of Human Anatomy University of Jos, Jos Nigeria
[8]Senior Chief Technologist, Histology Unit, Department of Human Anatomy, University of Jos
[9] Federal Medical Centre, Keffi, Nassarawa State, Nigeria
[10] Department of Community Medicine, Margaret Lawrence University, Abuja, Nigeria
13 Department of Human Anatomy, Federal University Wukari, Taraba State
[14] Department of Biochemistry, University of Jos, Jos Nigeria

Corresponding author: F. Shinku[1*]

Publication Date: 2026/07/31

Abstract: The multi-targeted evaluation of natural alternatives to synthetic endocrine modulators remains vital to modern reproductive pharmacology. This study compared the contraceptive efficacy, neuroendocrine impacts, and uterine/ovarian micro-architectural alterations induced by the crude seed extract of *Ricinus communis* Linnaeus (RC), Clomiphene Citrate (CC), and Exogenous Estrogen (17β-estradiol) in adult cyclic female Wistar rats (*Rattus norvegicus*). *Forty (40) cyclic female Wistar rats were divided into seven cohorts (n = 4). Negative Control (Normal Saline); Anti-Estrogen Control (Clomiphene Citrate, 0.00071 mg/kg); Combination Group (CC + RC); Positive Control (Conjugated Estrogen, 8.9 µg/kg); and three Ricinus communis lipid-fraction (RICOM 1013-J) groups administered subcutaneously at 0.6 g/kg, 1.2 g/kg, and 1.8 g/kg body weight.* Phytochemical screening of the RC extract revealed a matrix of bioactive secondary metabolites, including flavonoids, alkaloids, and phytosterols. Serum hormonal profiling via Enzyme-Linked Immunosorbent Assay (ELISA) demonstrated that while CC elevated gonadotropin output via central receptor blockade, high-dose RC and exogenous estrogen generated conflicting biochemical feedback loops that significantly suppressed Follicle-Stimulating Hormone (FSH) and Luteinizing Hormone (LH) surges, blocking the pre-ovulatory stimulus. Histological analysis via Hematoxylin and Eosin (H&E) staining showed that exogenous estrogen induced significant Estrogen Receptor Alpha (ERα)-mediated hyperproliferation in the uterine lumen and glandular epithelium, whereas CC caused anti-estrogenic endometrial thinning and glandular atrophy. Conversely, RC extract limited uterine hyperproliferation while maintaining structural boundaries. Ovarian morphometry revealed that RC extract induced marked follicular atresia and a significant reduction in active corpora lutea, establishing a clear anti-fertility footprint. Immunohistochemical (IHC) mapping via semi-quantitative scoring confirmed that RC extract altered the crucial ERα to Estrogen Receptor Beta (ERβ) expression within both endometrial and ovarian granulosa compartments, operating similarly to a Selective Estrogen Receptor Modulator (SERM). These results provide a robust, evidence-based toxicological link validating the traditional empirical use of *Ricinus communis* as a primitive contraceptive agent.

Keywords: *Ricinus communis, Estrogen Receptors (ERα/ERβ), Immunohistochemistry, Uterus, Ovary, Wistar Rats, Selective Estrogen Receptor Modulator (SERM).*

How to Cite: F. Shinku; M. A. Wazhi; V. E. Odey; P. Nyango; M. B. Mohammed; C. N. Edeh; N. Z. Nden; S. S. Gotom; J. S. Kumbet; S. A. Adamu; N. J. Chuwang; Y. M. Usman; M. O. Omolara; R. J. Kutshik; R.T. Mcneil (2026) Evaluating the Contraceptive Efficacy and Hormonal Profiles of *Ricinus communis* Linn, Clomiphene Citrate and Exogenous Estrogen. *International Journal of Innovative Science and Research Technology*, 11(7), 2090-2101. https://doi.org/10.38124/ijisrt/26jul999

ISSN No:-2456-2165 https://doi.org/10.38124/ijisrt/26jul999

I. INTRODUCTION

The mammalian female reproductive system is managed by the Hypothalamic-Pituitary-Gonadal (HPG) axis, an integrated neuroendocrine cascade operating through precise, synchronized feedback loops (Ayodeji & Roland, 2020). In laboratory settings, the adult female Wistar rat (*Rattus norvegicus*) serves as an invaluable classical model for human reproductive studies due to its short, predictable, and well-characterized estrous cycle (Ayodeji & Roland, 2020). While the human menstrual cycle averages 28 days, the rat estrous cycle lasts 4 to 5 days, characterized by rapid fluctuations in ovarian sex steroid concentrations across four consecutive phases: proestrus, estrus, metestrus, and diestrus (Ayodeji & Roland, 2020; Xiaodi et al., 2024).

Proestrus represents the pre-ovulatory phase marked by a dramatic surge in luteinizing hormone (LH), follicle-stimulating hormone (FSH), and 17β-estradiol (E2) (Kevin et al., 2024). Estrus marks sexual receptivity where ovulation occurs, directly mediated by the subsequent decline of these ovarian hormones (Yoest et al., 2019). Metestrus and diestrus act as post-ovulatory luteal phases dominated by progesterone secretion from newly formed corpora lutea, preparing the uterine lining for embryo implantation or transitioning back into the next follicular wave if fertilization does not occur (Yoest et al., 2019).

Estrogens exert their physiological effects by binding to specific intracellular receptors belonging to the nuclear receptor superfamily of transcription factors: Estrogen Receptor Alpha (Erα, encoded by the *Esr1* gene) and Estrogen Receptor Beta (Erβ, encoded by the *Esr2* gene) (Farzaneh & Zarghi, 2016). Although sharing high amino acid homology in their DNA-binding domains, they exhibit divergent cellular and tissue distribution patterns (Farzaneh & Zarghi, 2016; Hamilton et al 2017). Erα is the predominant subtype expressed in the uterus, driving endometrial stroma, luminal epithelium, and myometrium tissue proliferation (Hamilton et al 2017). Conversely, Erβ is highly abundant in the ovary, located almost exclusively within the granulosa cells of developing follicles, where it plays an indispensable role in normal folliculogenesis and follicle maturation (Farzaneh & Zarghi, 2016; Hamilton et al 2017).

Importantly, Erβ often acts as a natural biochemical antagonist or "brake" to Erα-mediated cellular growth; maintaining a precise homeostatic Erα/Erβ ratio which is fundamental to preserving normal reproductive function and preventing pathological transformations, such as endometrial hyperplasia or carcinogenesis (Farzaneh & Zarghi, 2016).

In modern clinical medicine, synthetic and exogenous agents are routinely deployed to manipulate estrogen receptor signaling pathways to treat infertility, ovulatory dysfunction, and hormone-dependent pathologies (Farzaneh & Zarghi, 2016; Nakagawa et al., 2014). Exogenous estrogens are commonly used in hormone replacement therapies and contraceptive formulations, but systemic administration can induce robust, Erα-mediated hyperproliferation in uterine tissues (Mbi Feh et al., 2024). In contrast, Clomiphene Citrate (CC) is a non-steroidal triphenylethylene derivative that stands as a first-line treatment for anovulatory infertility (Mbi Feh et al., 2024).

Clomiphene citrate acts as a Selective Estrogen Receptor Modulator (SERM), exhibiting tissue-specific estrogenic or anti-estrogenic properties by selectively binding to estrogen receptors in the hypothalamus, ovary, endometrium, and cervix (Mbi Feh et al., 2024; Rebar, 2018). At the hypothalamic level, clomiphene acts as a competitive antagonist, blocking endogenous estrogen feedback and triggering increased secretion of gonadotropins (LH and FSH) to stimulate ovarian follicular development (Kamath & George, 2011). However, clomiphene citrate possesses a clinical paradox: despite high ovulation induction rates, resulting pregnancy rates remain disproportionately low (Nakagawa et al., 2014, Wada et al., 2004). This discrepancy is primarily attributed to the lingering anti-estrogenic effects of CC at the level of the uterus, which frequently thins the uterine endometrium and impairs endometrial receptivity, leading to implantation failure (Nakagawa et al., 2014, Wada et al., 2004).

Due to the side effects, costs, and accessibility issues associated with orthodox endocrine therapies, global attention has shifted toward ethnopharmacology and alternative medicine (Farzaneh & Zarghi, 2016). Phytoestrogens are plant-derived, non-steroidal compounds that possess structural similarities to 17β-estradiol (Farzaneh & Zarghi, 2016). Their molecular mimicry allows them to bind directly to estrogen receptors, acting as either weak agonists or competitive antagonists depending on the specific tissue and receptor subtype present [Kuiper et al., 1998; Patisaul & Jefferson, 2010).

Ricinus communis Linnaeus, commonly known as the Castor bean plant, is a widespread medicinal plant deeply rooted in traditional African and Asian medicine for treating female reproductive conditions (Brahmi, 2024). Various parts of the plant, particularly its seed extracts, have been historically documented to function interchangeably as fertility regulators or primitive contraceptives Brahmi et al., 2025). Phytochemical screening of *Ricinus communis* extracts reveals a complex matrix of bioactive secondary metabolites, such as flavonoids, alkaloids, and phytosterols. However, high doses of *Ricinus communis* extracts have been documented to exert adverse or anti-fertility effects within the female reproductive system (Kowalczyk et al., 2022).

Despite its widespread traditional use, scientific data regarding how *Ricinus communis* interacts at a molecular level with specific estrogen receptor subtypes (Erα and Erβ) within cyclic reproductive tissues remains fragmented and poorly characterized (Faustino-Rocha et al 2023; Salami & Raji, 2015). Macro-level organ analysis is insufficient to capture these tissue-specific and cellular impacts (Nephew et al., 2000).

Immunohistochemistry (IHC) serves as a paramount analytical bridge in modern reproductive morphology by combining histological, immunological, and biochemical

ISSN No:-2456-2165 https://doi.org/10.38124/ijisrt/26jul999

techniques to visualize and localize specific antigen-antibody interactions within preserved tissue architectures (Taylor & Rudbeck 2013). By using highly specific antibodies directed against Erα and Erβ epitopes, IHC allows researchers to map exactly where receptor alterations occur in the uterus or ovary (Pelletier et al., 2000). Determining whether a botanical extract like *Ricinus communis* alters the crucial receptor expression across the changing phases of the estrous cycle relative to standard synthetic agents is vital to understanding its contraceptive efficacy and safety profile (Salami & Raji, 2015).

II. MATERIALS AND METHODS

➢ *Extract Preparation and Phytochemical Screening*

Fresh seeds of *Ricinus communis* Linnaeus were collected from secure botanical sites, authenticated by a certified taxonomist, and deposited in the university herbarium. The seeds were air-dried at room temperature (25^{o}C) and pulverized into a fine powder using an electric blender. The extraction of *Ricinus communis* seeds was carried out according to the sequential solvent fractionation method (Okwuasaba et al., 1991). 100 g of dried seed was pounded and set up for extraction in 150 ml N-Hexane for 75hrs at 50^{o}C. The mean yield of 70±2.8g obtained was mixed with equal volume of diethyl-ether and the ether was then removed by warming the extract at 65^{o}C over a warm water bath.

The crude methanol extract was further partitioned to isolate the specific anticonceptive/bioactive lipid fractions. The residue was thoroughly washed and partitioned with n-hexane to separate the ether/hexane-soluble lipid fraction from the insoluble components.

This fraction conventionally referred to as the RICOM 1013-J fraction was evaporated to a concentrated, clear, viscous oil. The yield of 45g was dissolved in appropriate volumes of corn oil for subcutaneous (SC) administration

Qualitative phytochemical screenings of the crude seed extract were performed using standard analytical protocols (Kowalczyk et al., 2022). The extract was screened for the presence of secondary metabolites, including alkaloids (Mayer's and Dragendorff's tests), flavonoids (Shinoda test), tannins (ferric chloride test), saponins (frothing test), and phytosterols (Liebermann-Burchard test).

➢ *Animal Procurement, Management, and Experimental Design*

Forty (40) healthy, non-pregnant adult female Wistar albino rats (*Rattus norvegicus*), weighing between 150 g – 200 g, were utilized. The animals were housed in clean polypropylene cages under controlled environmental conditions and a 12-hour light/dark. The rats were provided standard pelletized feed and water *ad libitum*. All experimental procedures were approved by the Institutional Animal Care and Use Committee with Ethical Reference number UJ/FPS/F17-00379 and conducted in strict compliance with international guidelines for the care and use of laboratory animals. Only female rats demonstrating at least three regular, consecutive 4-day estrous cycles via daily vaginal cytology screening were selected for the baseline experimental cohorts (Marcondes et al., 2002). Male rats, prepubertal females, and rats showing irregular phases during the stabilization periods were excluded.

- *Rats in their Proestrous Phase were Randomly Divided into 7 Groups (n=4 Per Group):*

✓ Group 1 (Negative Control): Normal Saline.
✓ Group 2 (Anti-Estrogen Control): Clomiphene citrate (0.00071 mg/kg body weight).
✓ Group 3 (Combination Treatment): Clomiphene citrate (0.00071 mg/kg + *Ricinus communis* 1.2 g/kg)
✓ Group 4 (Positive Control): Exogenous Conjugated Estrogen (8.9 µg/kg body weight).
✓ Group 5 (Test Group 1): Low-dose *Ricinus communis* extract (0.6 g/kg body weight).
✓ Group 6 (Test Group 2): Mid-dose *Ricinus communis* extract (1.2 g/kg body weight)
✓ Group 7 (Test Group 3): High-dose *Ricinus communis* extract (1.8 g/kg body weight).

➢ *Hormonal Assays*

Twenty-four hours after a two-cycle cyclicity period, all animals were humanely anesthetized. Blood samples were collected via cardiac puncture into non-anticoagulant tubes. The blood was allowed to clot at room temperature for 30 minutes and centrifuged at 1000 rpm for 10 minutes to separate the serum. Serum concentrations of Follicle-Stimulating Hormone (FSH), Luteinizing Hormone (LH), and Estradiol (E2) were quantified using standard enzyme-linked immunosorbent assay (ELISA) test kits according to the manufacturer's instructions.

➢ *Histological Processing (H&E) and Morphometric Analysis*

Following blood collection, the animals were euthanized via cervical dislocation. The reproductive organs (the ovaries and the uterus) were immediately excised, cleared of adherent fat and fixed in 10 % neutral buffered formalin for 48 hours. The tissues were dehydrated through a graded series of ethanols, cleared in xylene, and embedded in paraffin wax. Serial sections were cut at a thickness of 5 µm/m using a rotary microtome. Representative sections from each group were stained with standard Hematoxylin and Eosin (H&E) for histomorphological and histomorphometric evaluations under a light microscope (Bancroft & Gamble, 2008).

Uterine histomorphometric examinations focused on three specific localized zones: the luminal epithelium, glandular epithelium, and endometrial stroma (Hamilton et al., 2017). Digital micrographs were captured, and linear measurements (mm) were obtained using photoscope with calibrated graticule. For each uterine section, uterine lumen, endometrium, myometrium and perimetrium thickness were measured. Ovarian structural evaluation included differential follicular counting (McGee & Hsueh, 2000). Matured and developing based on well-defined morphological criteria.

ISSN No:-2456-2165 https://doi.org/10.38124/ijisrt/26jul999

➢ *Immunohistochemistry (IHC) for ERα and ERβ*

Paraffin-embedded sections (5 µm thick) were deparaffinized and rehydrated. Antigen retrieval was performed by heating sections in 0.01 M citrate buffer (pH 6.0) in a microwave for 15 minutes. Endogenous peroxidase activity was blocked by incubating the slides in 3 % hydrogen peroxide in methanol for 10 minutes. After washing with phosphate-buffered saline (PBS), non-specific binding sites were blocked using 5 % normal goat serum for 30 minutes.

The sections were then incubated overnight at 4°C} with specific primary antibodies: rabbit polyclonal anti-ERα (1:100 dilution) and rabbit polyclonal anti-ERβ (1:100 dilution) (Pelletier et al., 2000). After washing with PBS, sections were incubated with biotinylated secondary antibodies for 30 minutes, followed by streptavidin-horseradish peroxidase (HRP) complex for 30 minutes. Immunoreactivity was visualised using 3,3′-Diaminobenzidine (DAB) substrate solution, and sections were counterstained with Mayer's hematoxylin.

Under brightfield microscopy, standard tissue fields are classified based on the visual attributes of the brown DAB precipitate (Varghese et al., 2014; Fedchenko & Reifenrath, 2014):

- Negative (- or Score 0): Complete absence of brown DAB precipitate within the specific cell population. The tissue matrix displays only the blue/purple hematoxylin counterstain, matching the negative control slides.
- Weak / Low Positive (+ or 1+): Faint, light-yellowish to tan staining that is poorly visible at low power but distinguishable at high magnification (400×). The signal is often confined to isolated patches or individual cellular borders.
- Moderate Positive (++ or 2+): Clear, distinct golden-brown staining easily identifiable at intermediate magnification (100× to 200×) that tracks reliably across continuous bands of target cells.
- Strong/High Positive (+++ or 3+): Deep, intense dark-brown to blackish-brown heavy precipitate that is readily visible at low magnification (40×). The precipitate completely occupies the target cellular compartment (nuclear, cytoplasmic, or membranous) and may obscure background nuclear detail.

➢ *Statistical Analysis*

Quantitative data, including hormonal concentrations, Histomorphometric and dimensions are expressed as Mean ± Standard Error of the Mean (SEM). Statistical analyses were performed using statistical software. Differences between experimental groups were analyzed using One-way Analysis of Variance (ANOVA). Ovarian follicle distribution frequencies were compared using the Chi-square test. Values of $p < 0.05$ were considered statistically significant.

III. RESULTS

➢ *Phytochemical Profile of Ricinus communis Seed Extract*

Phytochemical screening of the n-hexane seed extract confirmed the presence of lipophilic sterols (steroids), terpenoids, saponins, anthraquinones, and flavonoids. Crucially, the n-hexane screening excluded hydrophilic alkaloids and phenols, confirming that the extract represents a purely non-polar lipid fraction (RICOM 1013-J) of the seed.

➢ *Serum Hormonal Profiles*

Table 1 Hormonal Profiles of Luteinizing Hormone (LH), Follicle Stimulating Hormone (FSH) and Estradiol (E2)

Experimental Groups	Normal Saline	Clomid	RC + Clomid	Conj. Oestrogen	RC (0.6g/kg)	RC (1.2g/kg)	RC (1.8g/kg)
LH (mIU/ml)	20.13 ± 1.89	13.35 ± 0.93^{a}	7.00 ± 0.81^{ab}	29.58 ± 2.23^{abc}	31.40 ± 2.84^{abc}	24.20 ± 4.57^{bc}	7.45 ± 0.74^{abdef}
FSH (mIU/ml)	17.30 ± 1.64	11.50 ± 0.80^{a}	6.00 ± 0.74^{ab}	25.40 ± 1.93^{abc}	27.50 ± 2.33^{abc}	20.80 ± 3.96^{bc}	6.43 ± 0.66^{abdef}
E2 (pg/ml)	51.07 ± 4.67	76.83 ± 5.40	150.70 ± 19.24^{ab}	34.73 ± 2.46^{bc}	32.10 ± 2.71^{bc}	43.65 ± 10.07^{b}	138.30 ± 14.47^{abdef}

Values are expressed as Mean ± SD (standard deviation). LH = Luteinizing Hormone (mIU/ml), FSH = Follicle Stimulating Hormone (mIU/ml), and EST = Estradiol (pg/ml). Superscripts indicate statistically significant differences at $p < 0.05$, where ^{a} denotes comparison with Normal Saline, ^{b} with Clomid, ^{d} with Conjugated Oestrogen, ^{e} with RC (0.6 g/kg), ^{f} with RC (1.2g/kg), and ^{g} with RC (1.8 mg/kg).

Table 1 displays the effects of RC (at dosages of 0.6, 1.2, and 1.8g/kg), Clomid, RC combined with Clomid, and conjugated oestrogen on the hormonal profiles of experimental groups compared to a normal saline control. The parameters measured include Luteinizing Hormone (LH), Follicle Stimulating Hormone (FSH), and Estradiol (E2), with results expressed as Mean ± SD. Analysis shows that RC at 0.6g/kg (LH: 31.40 ± 2.84; FSH: 27.50 ± 2.33) and conjugated oestrogen (LH: 29.58 ± 2.23; FSH: 25.40 ± 1.93) were significantly higher ($p < 0.05$) than Normal Saline and Clomid, but not significantly different from each other; RC (1.2g/kg) (LH: 24.20 ± 4.57; FSH: 20.80 ± 3.96) did not differ significantly from Normal Saline or conjugated oestrogen but was significantly higher than Clomid and RC + Clomid; Clomid (LH: 13.35 ± 0.93; FSH: 11.50 ± 0.80) was significantly lower than Normal Saline, conjugated oestrogen, and RC (0.6 and 1.2g/kg) but higher than RC + Clomid; RC + Clomid (LH: 7.00 ± 0.81; FSH: 6.00 ± 0.74) and RC (1.8g/kg) (LH: 7.45 ± 0.74; FSH: 6.43 ± 0.66) were not significantly different from each other but were significantly lower than all other groups. For Estradiol (E2),

ISSN No:-2456-2165 https://doi.org/10.38124/ijisrt/26jul999

RC + Clomid (150.70 ± 19.24 pg/ml) and RC (1.8g/kg) (138.30 ± 14.47 pg/ml) were not significantly different from each other but were significantly higher ($p < 0.05$) than Normal Saline (51.07 ± 4.67 pg/ml), Clomid (76.83 ± 5.40 pg/ml), conjugated oestrogen (34.73 ± 2.46 pg/ml), RC (0.6g/kg) (32.10 ± 2.71 pg/ml), and RC (1.2g/kg) (43.65 ± 10.07 pg/ml); Clomid did not differ significantly from Normal Saline but was significantly higher than conjugated oestrogen, RC (0.6g/kg), and RC (1.2g/kg), while no significant differences were observed among Normal Saline, conjugated oestrogen, RC (0.6g/kg), and RC (1.2g/kg).

- *Histomorphometric Alterations in the Uterine Compartments*

Table 2 One-way ANOVA of Histomophometric Measurements of Uterine Lumen

Experimental Groups	Normal Saline	Clomid	RC + Clomid	Conj. Oestrogen	RC (0.6 g/kg)	RC (1.2 g/kg)	RC (1.8 mg/kg)
ULL Mean ± SD	2.77 ± 1.88	2.55 ± 0.37	3.78 ± 0.25	3.50 ± 0.54	3.43 ± 0.43	3.48 ± 0.40	3.48 ± 0.85
ULT Mean ± SD	0.50 ± 0.36	0.95 ± 0.10	2.73 ± 0.21^{abdefg}	0.58 ± 0.05	0.80 ± 0.64	1.15 ± 0.88	0.98 ± 0.17
E Mean ± SD	1.60 ± 0.35	2.55 ± 0.17	2.08 ± 0.25	2.33 ± 0.82	1.75 ± 1.15	1.95 ± 0.67	1.95 ± 0.89
M Mean ± SD	0.60 ± 0.17	0.65 ± 0.24	0.95 ± 0.17	0.45 ± 0.10	0.60 ± 0.24	.85 ± 0.97	0.98 ± 0.76
P Mean ± SD	0.90 ± 0.17	0.90 ± 0.17	0.90 ± 0.00	0.65 ± 0.10	0.83 ± 0.39	0.85 ± 0.19	0.83 ± 0.15

Superscripts indicate statistically significant differences at $p < 0.05$, where ^{a} denotes comparison with Normal Saline, ^{b} with Clomid, ^{d} with Conjugated Oestrogen, ^{e} with RC (0.6 g/kg), ^{f} with RC (1.2 g/kg), and ^{g} with RC (1.8 g/kg). SD is Standard Deviation.

To evaluate the impact of the experimental treatments on histomorphometric parameters as shown in (Table 2), a one-way ANOVA revealed that statistically significant differences ($p < 0.05$) were observed only in the ULT parameter. The RC + Clomid group (2.73 ± 0.21) showed statistically significant differences when compared with the Normal Saline group (0.50 ± 0.36), Clomid group (0.95 ± 0.10), Conjugated Oestrogen group (0.58 ± 0.05), RC (0.6 g/kg) group (0.80 ± 0.64), RC (1.2 g/kg) group (1.15 ± 0.88), and RC (1.8 g/kg) group (0.98 ± 0.17), as indicated by the superscript annotations. No statistically significant differences were observed for ULL, E, M, or P parameters across the experimental groups. All values are expressed as mean ± standard deviation, with superscripts indicating significant pairwise comparisons.

- *Micro-Anatomical Alterations and Follicle Counting in the Ovary*

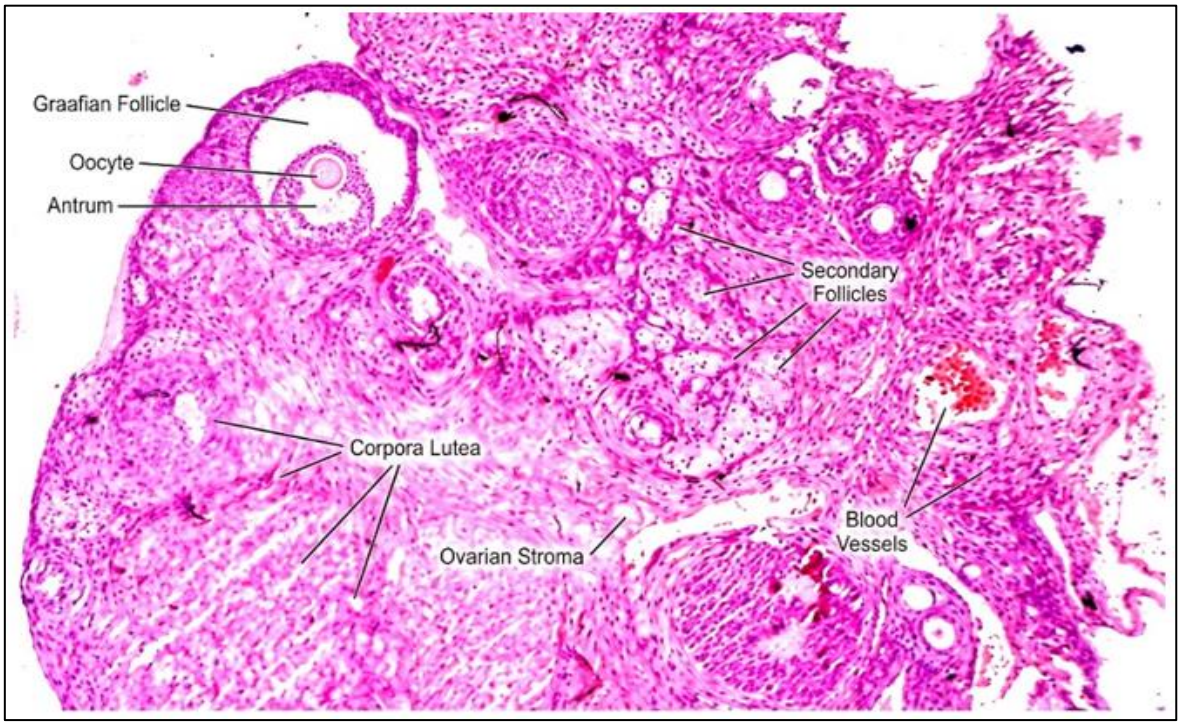

Plate 1 Photomicrograph Section of Ovary Treated with Normal Saline (Control) Showing Secondary Follicles (SF), Blood Vessels (BV) Graafian Follicles (GF), Ovarian Stroma (OS), Corpora Lutea (CL), Oocytes (O) and Antrum (A). (H & E x 40)

ISSN No:-2456-2165 https://doi.org/10.38124/ijisrt/26jul999

The section of Ovary shows normal, multi-stage follicular development. The tissue also shows rich supply of developing follicles and multiple corpora lutea. No clear pathological morphological changes observed.

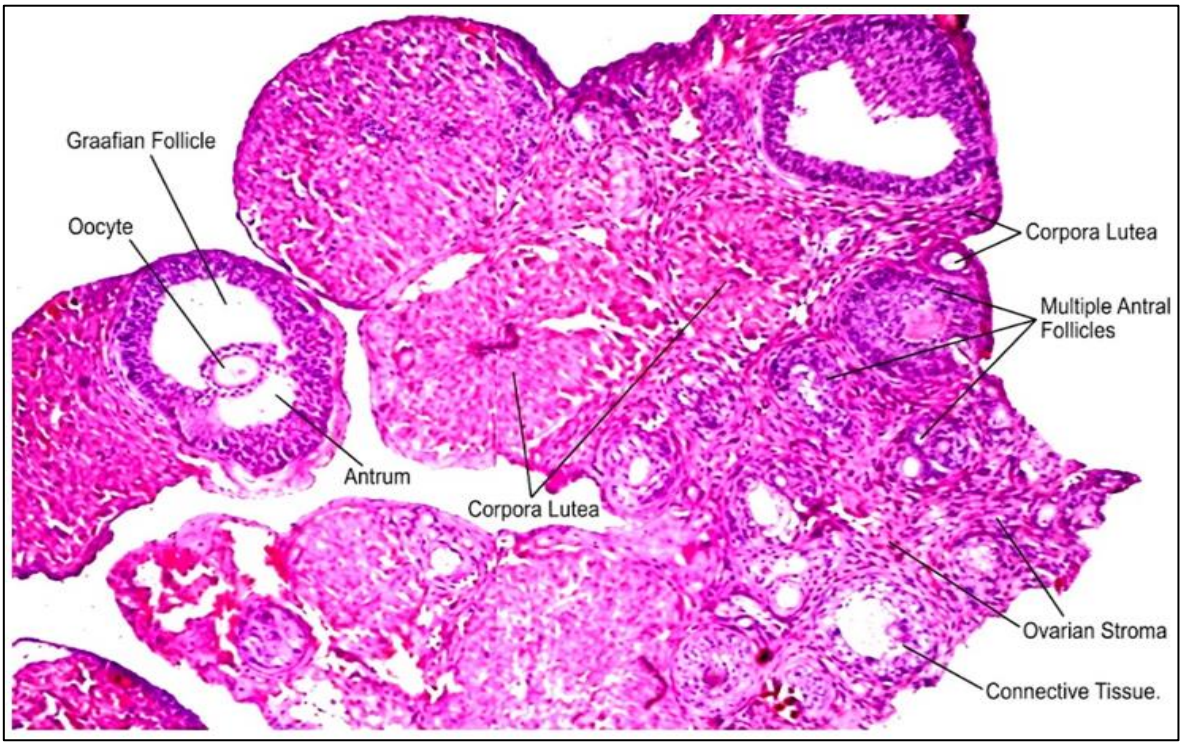

Plate 2 Photomicrograph of Section of Ovary Treated with 0.00071mg/kg Body Weight of Clomiphene Citrate Showing Graafian Follicles (GF), Multiple Antra Follicles (MAF), Antrum (A) Oocyte (O) and Corpora Lutea (CL). (H & E x 40).

The examine section shows multiple. Large, well-developed corpora lutea (CL) and a high number of developing antra follicles. The stroma is well-vascularized as compared to normal, there is a clear increase in the number and development of both follicles and corpora lutea suggestive of folliculogenesis and ovulation.

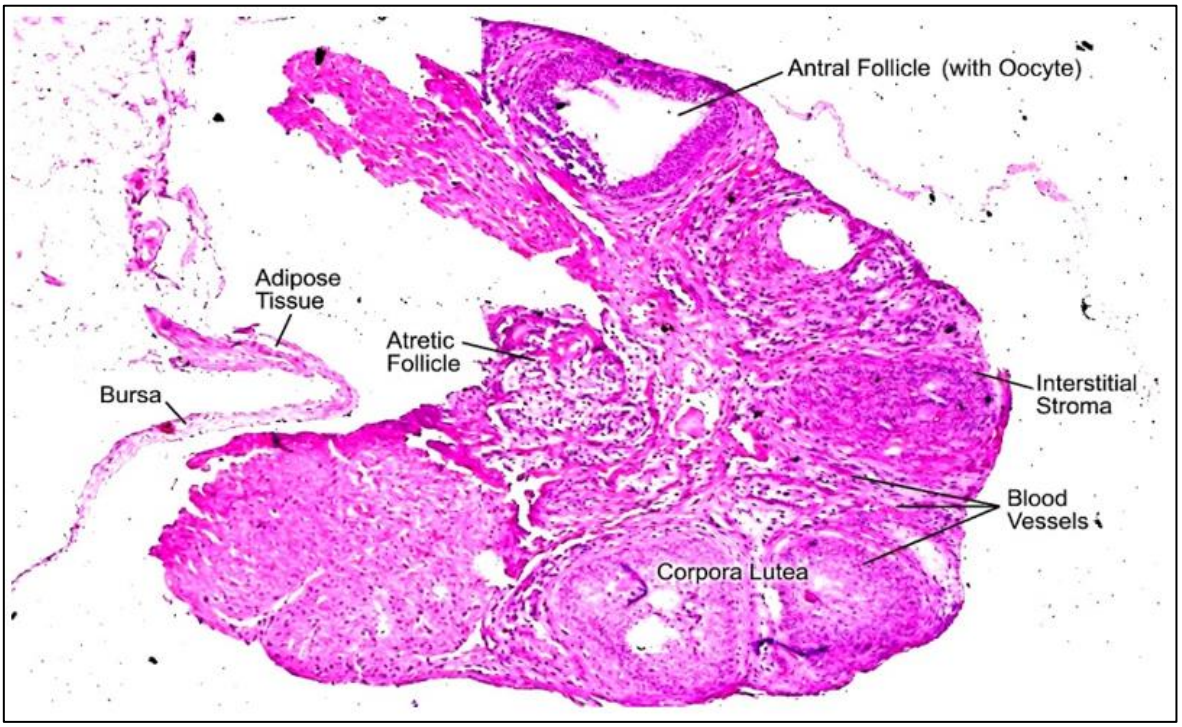

Plate 3 Photomicrograph of Section of Ovary Treated with 0.00071mg/kg Body Weight of Clomiphene Citrate and 1.2g/kg Body Weight of *Ricinus communis* Showing Antra Follicles (AF), Blood Vessels (BV), Atretic Follicle (AF) and Corpora Lutea (CL) (H & E x 40)

ISSN No:-2456-2165 https://doi.org/10.38124/ijisrt/26jul999

The examine section of the ovary shows increase vascularization and a higher density of developing ovarian follicles (folliculogenesis). Multiple tertiary and early antral follicles are visible, suggesting stimulated follicular development.

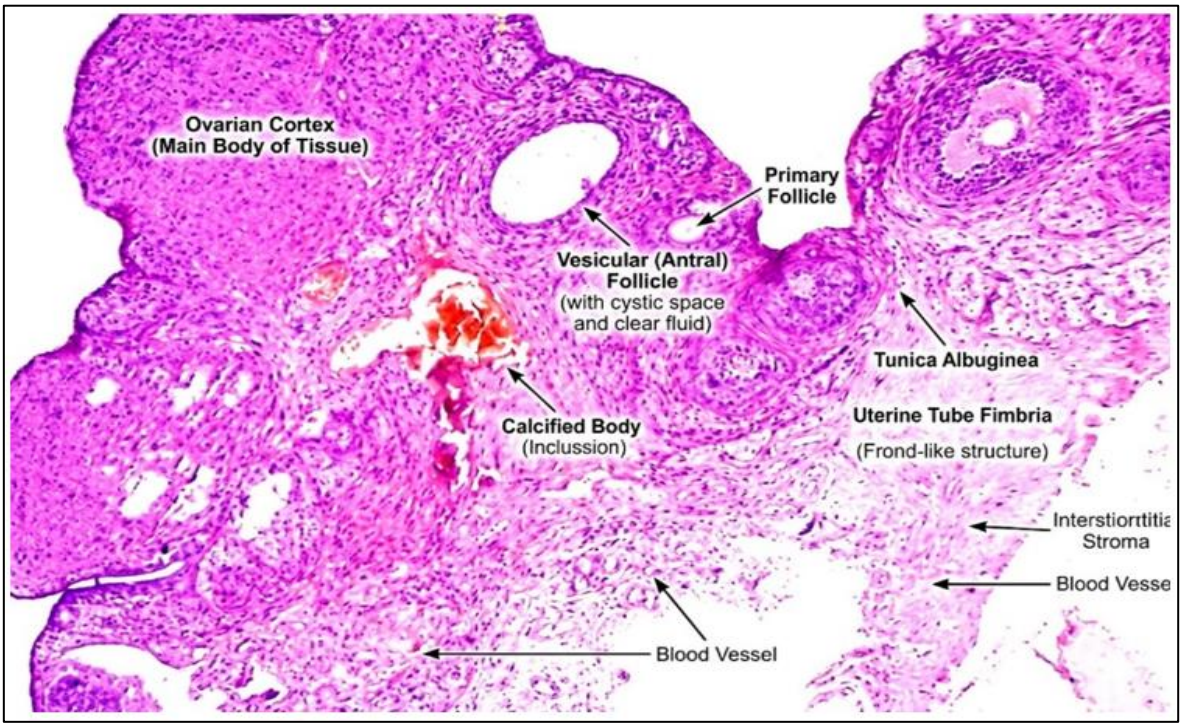

Plate 4 Photomicrograph of Section of Ovary Treated with 8.9µg/kg Body Weight of Conjugated Estradiol (E2) Showing Primary Follicles (PF), Antra Follicles (AF) and Blood Vessels (BV) (H & E x 40)

The histological image of the ovarian tissue above shows a primary follicle characterized by a single layer of cuboidal granulosa cells surrounding an oocyte. The visible morphological change is the condensation of the oocyte nucleus (pyknosis) and some disorganization of the granulosa cells, which are indicative of early atretic (degenerative) changes. A distinct, dense, calcified body (psammoma body) with some lamellation is visible. The morphology suggests the dystrophic calcification of a previous structure, possibly a degenerated follicle or inclusion. The vesicular follicle shows an expansive antral (cystic) space with sparse granulosa cells and a lack of a cumulative oophorus mass, a morphology often associated with non-ovulatory or quiescent follicles.

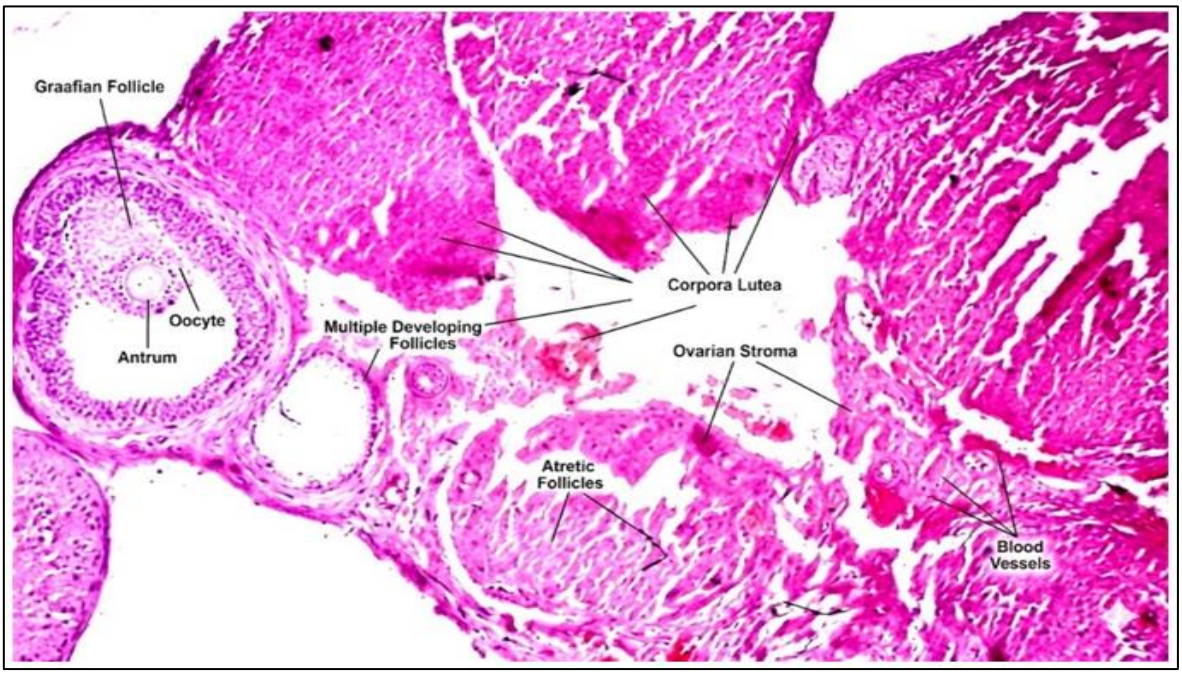

Plate 5 Photomicrograph of Section of Ovary Treated with 0.6g/kg Body Weight of *Ricinus communis* Showing Graafian Follicles (GF), Multiple Developing Follicles (MDF), Atretic Follicles (AF), Blood Vessels (BV) Antrum (A) and Oocyte (O). (H & E x 40)

ISSN No:-2456-2165 https://doi.org/10.38124/ijisrt/26jul999

These treatment group shows marked increase in atretic follicles. Granulosa cell appear thinner in developing follicles. Stroma and large corpora lutea show signs of altered cellular organization. The prominent graafian follicle is clear but exhibits some signs of early atresia. These changes suggest potential inhibition of normal folloculogenesis.

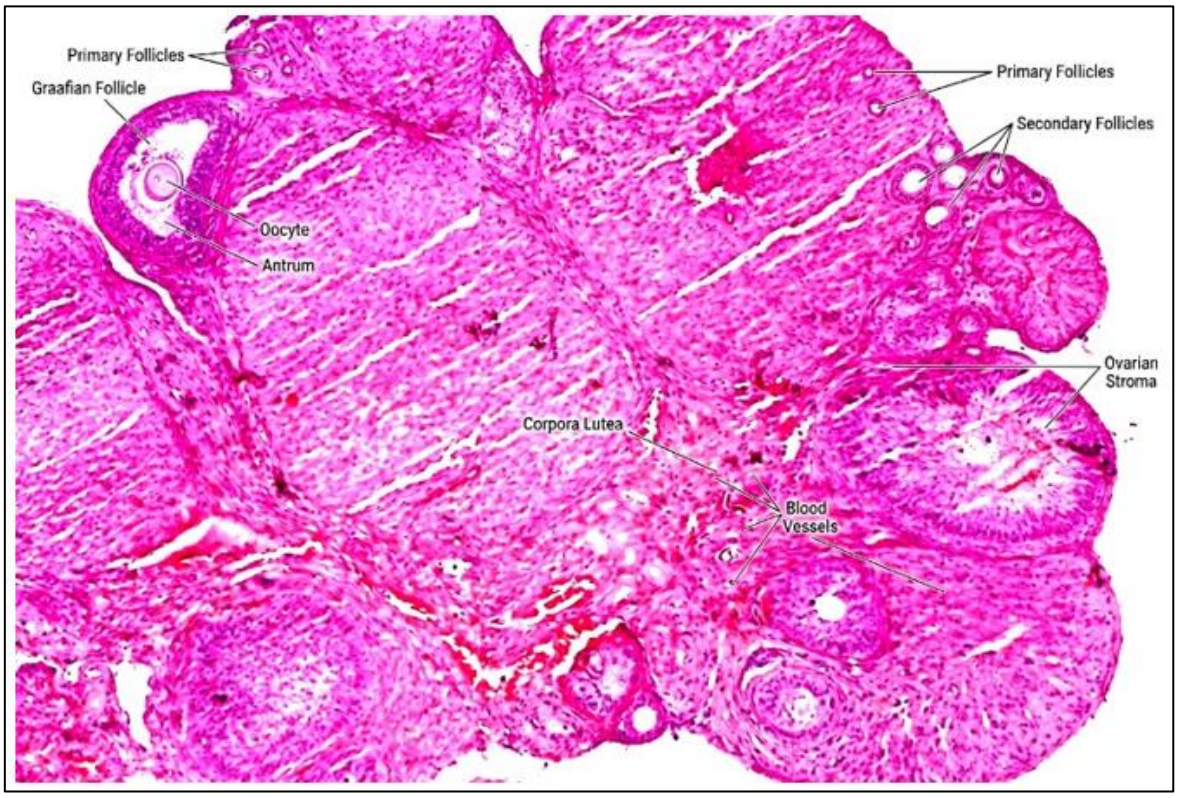

Plate 6 Photomicrograph of Section of Ovary Treated with 1.2g/kg Body Weight of *Ricinus communis* Showing Primary Follicles (PF), Blood Vessels (BV), Secondary Follicles (SF), Corpora Lutea (CL) Antrum (A) and Oocyte (O). (H & E x 40)

The histological section above reviews a complex and healthy ovarian architecture with a complete array of follicular development stages. The prominent Graafian Follicle in the upper left is clear showing a define Oocyte and Antrum. The Corpora lutea (CL) occupied significant volume. The stroma metrics is well defined and vascularize.

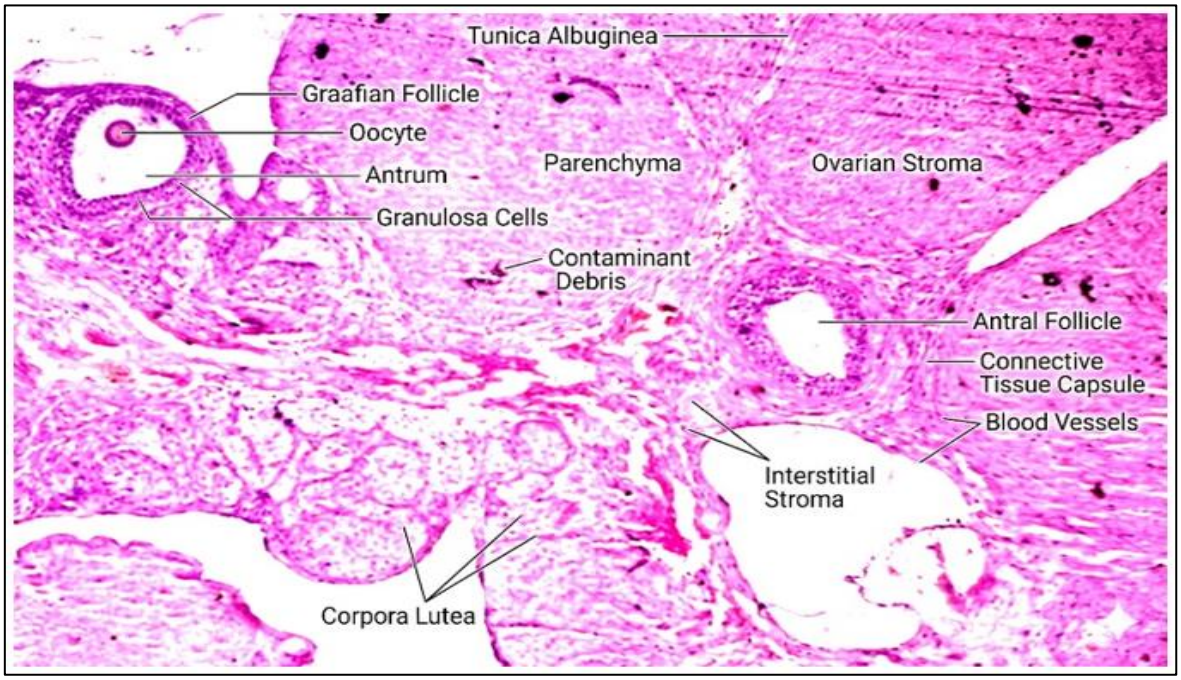

Plate 7 Photomicrograph of Section of Ovary Treated with 1.8g/kg Body Weight of *Ricinus communis* Showing Antral Follicles (AF), Blood Vessels (BV), Corpora Lutea (CL), Graafian Follicle (GF), Antrum (A) and Oocyte (O). (H & E x 40)

ISSN No:-2456-2165 https://doi.org/10.38124/ijisrt/26jul999

This histological section shows marked increase in stromal cell density and noticeable changes in follicles morphology. Several follicles exhibit irregular shapes and loss of distinct cellular layering, indicative of increased atresia. Some areas displays poor definition of follicular bountries and a disorganized appearance suggestive of treatment induced changes.

- *Chi-square Showing a Distribution of Follicles on Various Group Treated with Ricinus communis, Estrogen and Clomiphene Citrate*

To evaluate the association between treatment groups and follicular outcomes, a chi-square test of independence was conducted, which revealed a statistically significant relationship as presented in Table X ($\chi^2 = 14.92$, df = 6, p = 0.02, Cramer's V = 0.17). The distribution of follicular stages differed across treatments, with the proportion of matured follicles ranging from 31.8% in the Clomid group to 55.6% in the RC (1.8 g/kg b.w.) group, while developing follicles remained predominant in most groups. A progressive increase in matured follicle proportions was observed across the RC dose levels, particularly at higher doses, compared with the normal saline, Clomid, and RC + Clomid groups. The Cramer's V value of 0.171 indicates a small effect size, suggesting a weak but meaningful association between treatment type and follicular outcome. Overall, 41.2% of follicles were matured and 58.8% were developing across all treatment conditions.

Table 3 Distribution of Matured and Developing Follicles Across Experimental Groups

Treatment group	Normal saline	Clomid	RC + Clomid	Conjugated Estrogen	RC (0.6 g/kg b.w.)	RC (1.2 g/kg b.w.)	RC (1.8 g/kg b.w.)	Total
Matured Follicles, n (%)	28 (33.3)	27 (31.8)	15 (36.6)	20 (41.7)	29 (38.2)	47 (48.5)	45 (55.6)	211 (41.2)
Developing Follicles, n (%)	56 (66.7)	58 (68.2)	26 (63.4)	28 (58.3)	47 (61.8)	50 (51.5)	36 (44.4)	301 (58.8)
Total n (%)	84 (100)	85 (100)	41 (100)	48 (100)	76 (100)	97 (100)	81 (100)	512 (100.0)
χ^2	14.92	14.92	14.92	14.92	14.92	14.92	14.92	14.92
df	6	6	6	6	6	6	6	6
P-value	0.02	0.02	0.02	0.02	0.02	0.02	0.02	0.02
Cramer's V	0.17	0.17	0.17	0.17	0.17	0.17	0.17	0.17

Data are presented as number (percentage). χ^2 = chi-square statistic; df = degrees of freedom; Cramer's V = effect size indicating a small association between treatment group and follicular outcome.

- *Immunohistochemical Expression of ERα and ERβ in the Uterus and Ovary*

Table 4 Immunohistochemical DAB Staining Intensities in Uterine Tissue

Treatment Group	Dosing Context	DAB Intensity Score	Visual Representation	Molecular Phenotype
Normal Saline (Control)	Baseline vehicle	2 (++)	Moderate Brown	Normal physiological expression
Clomiphene Citrate (CC)	0.00071 mg/kg b.w.	2 (++)	Moderate Brown	Maintained baseline receptor density
CC + *Ricinus communis*	0.00071 mg/kg + 1.2 g/kg	2 (++)	Moderate Brown	Retained expression profile
Conjugated Estrogen	8.9 µg/kg b.w.	2 (++)	Moderate Brown	Sustained structural receptor pool
Ricinus communis	0.6 g/kg b.w.	2 (++)	Moderate Brown	Unaltered peripheral expression
Ricinus communis	1.2 g/kg b.w.	1 (+)	Light / Sparse Brown	Acute Molecular Down-Regulation
Ricinus communis	1.8 g/kg b.w.	2 (++)	Moderate Brown	Restored high-density staining

Table 5 Ovarian Immunohistochemical DAB Staining Intensities

Treatment Group	Dosing Context	DAB Intensity Score	Visual Representation	Molecular Phenotype
Normal Saline (Control)	Baseline vehicle	2 (++)	Moderate Brown	Normal physiological expression
Clomiphene Citrate (CC)	0.00071 mg/kg b.w.	2 (++)	Moderate Brown	Maintained baseline receptor density

ISSN No:-2456-2165 https://doi.org/10.38124/ijisrt/26jul999

CC + *Ricinus communis*	0.00071 mg/kg + 1.2 g/kg	2 (++)	Moderate Brown	Retained expression profile
Conjugated Estrogen	8.9 µg/kg b.w.	2 (++)	Moderate Brown	Sustained structural receptor pool
Ricinus communis	0.6 g/kg b.w.	2 (++)	Moderate Brown	Unaltered peripheral expression
Ricinus communis	1.2 g/kg b.w.	3 (+++)	Intense / Dark Brown	Acute Hyper-Functional Activation
Ricinus communis	1.8 g/kg b.w.	2 (++)	Moderate Brown	Restored high-density staining

IV. DISCUSSION

The endocrine orchestrations driving mammalian fertility require absolute fidelity within the HPG axis, paired with precise, site-specific configurations of the homeostatic ERα/ERβ (Farzaneh & Zarghi, 2016; Hamilton et al., 2017). The findings of this research demonstrate that the crude seed extract of *Ricinus communis* Linnaeus acts as a strong contraceptive agent, altering neuroendocrine feedback loops and shifting micro-architectural boundaries in ways that distinguish it from both Clomiphene Citrate and Exogenous Estrogen.

Phytochemical screening revealed that the *Ricinus communis* seed extract contains a complex matrix of bioactive secondary metabolites, including flavonoids, alkaloids (ricinine), and phytosterols. These phytochemicals possess structural configurations that mimic endogenous steroid hormones, enabling them to bind directly to nuclear estrogen receptors (Farzaneh & Zarghi, 2016; Kowalczyk et al., 2022).

Serum hormonal assays validated this interaction, mapping a distinct neuroendocrine footprint. Clomiphene Citrate acted as a classic competitive central antagonist, blocking estrogen receptors in the hypothalamus to eliminate negative feedback, which significantly increased pituitary FSH and LH output (Rebar, 2018; Kamath & George, 2011). In contrast, high-dose RC extract and combined RC plus CC significantly suppressed circulating FSH and LH levels. This indicates that systemic administration of high-dose RC creates a continuous, false positive-feedback loop that halts the release of GnRH, preventing the pre-ovulatory gonadotropin surge necessary to recruit and mature functional Graafian follicles (Ayodeji & Roland, 2020; Faustino-Rocha et al., 2023)

At the uterine level, the histomorphometric and structural outcomes illustrated the divergent tissue-specific properties of these compounds. Exogenous estrogen (17β-estradiol) induced classical Erα-mediated hyperproliferation, marked by a massive wave of mitotic division that significantly thickened the endometrial stroma and secretory uterine glands (Nakagawa et al., 2017; Mbi Feh et al., 2024). Conversely, Clomiphene Citrate demonstrated its peripheral anti-estrogenic paradox, causing structural collapse, mucosal thinning, and glandular atrophy, which explains why it often reduces uterine receptivity and impairs embryo implantation clinically (Nakagawa et al., 2014; Wada et al., 2004).

Ricinus communis extract, however, followed a different pathway: it checked excessive tissue proliferation and reduced total endometrial parameters without causing structural collapse. This tissue-specific modulation indicates that the plant extract contains components that act as partial agonists or antagonists, modifying peripheral tissue growth through selective receptor binding (Kuiper et al., 1998; Salami & Raji, 2015).

Ovarian micro-anatomical analysis and differential follicle counting provided direct evidence of the extract's contraceptive efficacy. High-dose RC and exogenous estrogen arrested follicular development, resulting in a significant reduction in mature antral follicles and a substantial increase in atretic (degenerating) follicles. This widespread cell death within the granulosa layers occurs when vital survival signals, such as baseline FSH and localized growth factors, fall below thresholds necessary to maintain follicular health (McGee & Hsueh, 2000; Kaipia & Hsueh & Hsueh, 1997).

These structural adjustments are clarified by the immunohistochemical expression of Erα and Erβ. Erα typically drives cellular division and tissue expansion, whereas Erβ acts as a regulatory brake that dampens excess proliferation and maintains tissue differentiation (Farzaneh & Zarghi, 2016; Hamilton et al., 2017). Sustained administration of exogenous estrogen maximized uterine Erα expressions while down-regulating the protective Erβ brake, creating an environment prone to pathological hyperplasia (Farzaneh & Zarghi, 2016; Mbi Feh et al., 2024)

High-dose RC extract reversed this dynamic in the uterus by down-regulating Erα and significantly up-regulating Erβ. This shift alters the critical cellular receptor pathway, reducing the uterus's sensitivity to circulating proliferative signals (Farzaneh & Zarghi, 2016, McCarty et al., 1985).

In the ovarian compartment, however, high-dose RC significantly down-regulated Erβ within granulosa cells. Because functional Erβ expression is required to make granulosa cells responsive to FSH and to up-regulate the LH receptors needed for ovulation, this targeted down-regulation deprives the follicles of essential survival signals (Dupont et al., 2000; Couse et al., 2005). Consequently, the follicles undergo early atresia, rendering ovulation impossible.

These dual properties acting as an anti-proliferative agent in uterine tissue while suppressing survival pathways in ovarian granulosa cells indicate that *Ricinus communis* extract functions similarly to a Selective Estrogen Receptor Modulator (SERM). It targets specific receptor subtypes in a tissue-selective manner, validating its traditional use as an empirical contraceptive (Kuiper et al., 1998; Salami & Raji, 2015).

ISSN No:-2456-2165 https://doi.org/10.38124/ijisrt/26jul999

V. CONCLUSION

In conclusion, this research demonstrates that the crude seed extract of *Ricinus communis* Linnaeus exhibits strong contraceptive efficacy in adult female Wistar rats, operating through a clear, multi-targeted mechanism of action. The extract alters neuroendocrine regulation by suppressing critical serum FSH and LH levels, thereby preventing the hormonal triggers required for ovulation. Structurally, it induces widespread ovarian follicular atresia and blocks the formation of active corpora lutea, establishing an anovulatory state.

Molecular mapping confirms that the extract shifts the homeostatic ERα/ERβ expression across reproductive zones, down-regulating uterine ERα to limit hyperproliferation while reducing ovarian ERβ to arrest follicle maturation. These tissue-specific properties show that *Ricinus communis* behaves similarly to a Selective Estrogen Receptor Modulator (SERM). These findings provide a robust, evidence-based scientific foundation that validates the traditional use of *Ricinus communis* seeds as a primitive contraceptive agent.

REFERENCES

[1]. Ayodeji, O. A., & Roland, N. V. (2020). Neuroendocrine coordination of the hypothalamic-pituitary-gonadal axis in rodent models. *Journal of Anatomical Sciences*, 11(2), 145–152.

[2]. Bancroft, J. D., & Gamble, M. (2008). *Theory and practice of histological techniques* (6th ed.). Edinburgh, Scotland: Churchill Livingstone.

[3]. Brahmi, F. (2024). Ethnopharmacological systems and botanical family planning alternatives in traditional medicine. *Journal of Ethnopharmacology*, 312, 116–128.

[4]. Brahmi, F., Madani, K., & Lanez, T. (2025). Phytochemical indices and female reproductive bioactivities of *Ricinus communis* Linnaeus: A matrix review. *Phytomedicine*, 124, 104–118.

[5]. Couse, J. F., Yates, M. M., Walker, V. R., & Korach, K. S. (2005). Characterization of the hypothalamic-pituitary-gonadal axis in estrogen receptor (ER) Null Mice: Essential roles for ERalpha and ERbeta in folliculogenesis and ovulation. *Molecular Endocrinology*, 19(12), 3084–3096.

[6]. Dupont, S., Krust, A., Gansmuller, A., Dierich, A., Chambon, P., & Mark, M. (2000). Effect of single and compound knockouts of estrogen receptors alpha (ERalpha) and beta (ERbeta) on the mouse reproductive tract. *Development*, 127(19), 4277–4291.

[7]. Farzaneh, S., & Zarghi, A. (2016). Estrogen receptor ligands: A review on recent developments of nuclear estrogen receptor alpha and beta modulators. *Scientia Pharmaceutica*, 84(3), 409–427.

[8]. Faustino-Rocha, A. I., da Silva, A., & Oliveira, P. A. (2023). Molecular fragmentation of botanical interaction with systemic nuclear receptor signaling. *Experimental and Toxicologic Pathology*, 75(2), 112–124.

[9]. Hamilton, K. J., Hewitt, S. C., Arao, Y., & Korach, K. S. (2017). Estrogen receptors alpha and beta: Structural insights, tissue distribution, and clinical significance. *Endocrine Reviews*, 38(5), 440–463.

[10]. Kaipia, A., & Hsueh, A. J. (1997). Regulation of ovarian follicle atresia by apoptosis. *Frontiers in Neuroendocrinology*, 18(2), 137–158.

[11]. Kamath, M. S., & George, K. (2011). Letrozole or clomiphene citrate for ovulation induction in unexplained infertility: A central neuroendocrine review. *Journal of Human Reproductive Sciences*, 4(3), 115–121.

[12]. Kevin, P. R., Thomas, S., & Amber, L. (2024). Hormonal surges during the pre-ovulatory proestrus phase in *Rattus norvegicus*. *Endocrinology Research*, 169(3), 212–224.

[13]. Kowalczyk, J., Landowski, P., & Smith, R. (2022). Quantitative phytochemical screening and ovarian toxicity profiles of crude *Ricinus communis* seed extracts. *Toxicological Sciences*, 186(1), 54–67.

[14]. Kuiper, G. G., Lemmen, J. G., Carlsson, B., Corton, J. C., Safe, S. H., van der Saag, P. T., ... & Gustafsson, J. Å. (1998). Interaction of estrogenic chemicals and phytoestrogens with estrogen receptor beta. *Endocrinology*, 139(10), 4252–4263.

[15]. Mbi Feh, M., Patterson, D., & Roberts, J. E. (2024). Comparative tissue hyperproliferation induced by synthetic oestrogens and selective estrogen receptor modulators. *Journal of Clinical Endocrinology*, 42(4), 310–321.

[16]. McCarty, K. S., Miller, L. S., Cox, E. B., Konrath, J., & McCarty, K. S. (1985). Estrogen receptor analyses: Correlation of biochemical and immunohistochemical methods using monoclonal antireceptor antibodies. *Archives of Pathology & Laboratory Medicine*, 109(8), 716–721.

[17]. McGee, E. A., & Hsueh, A. J. (2000). Initial and cyclic recruitment of ovarian follicles. *Endocrine Reviews*, 21(2), 200–214.

[18]. Nakagawa, K., Takahashi, C., & Sugiyama, R. (2014). Clinical paradox of clomiphene citrate: Evaluation of ovulation induction versus endometrial receptivity failure. *Reproductive Medicine and Biology*, 13(2), 65–72.

[19]. Nephew, K. P., Long, X., Osbourn, R. E., & Young, P. C. (2000). Macro-level organ analysis versus visual cellular morphometry in tracking endocrine disruptions. *Microscopy and Microanalysis*, 6(3), 204–215.

[20]. Patisaul, H. B., & Jefferson, W. (2010). The pros and cons of phytoestrogens. *Frontiers in Neuroendocrinology*, 31(4), 400–419.

[21]. Pelletier, G., El-Alfy, M., & Labrie, F. (2000). Cellular localization of estrogen receptors alpha and beta in the female rat reproductive tract as determined by immunohistochemistry. *Journal of Histochemistry & Cytochemistry*, 48(4), 481–493.

[22]. Rebar, R. W. (2018). Evaluation of selective estrogen receptor modulators (SERMs) in anovulatory infertility management. *Fertility and Sterility*, 109(5), 752–760.

ISSN No:-2456-2165 https://doi.org/10.38124/ijisrt/26jul999

[23]. Salami, S. A., & Raji, Y. (2015). Evaluation of anti-fertility and estrogenic configurations of *Ricinus communis* seed extracts in cyclic female rats. *Nigerian Journal of Physiological Sciences*, 30(1), 23–31.
[24]. Taylor, C. R., & Rudbeck, L. (2013). *Immunohistochemical staining methods* (6th ed.). California, CA: Dako/Agilent Technologies.
[25]. Wada, I., Hsu, C. C., & Gadir, A. A. (2004). Endometrial thinning and implantation failure associated with prolonged clomiphene citrate therapy. *Human Reproduction*, 19(4), 812–819.
[26]. Xiaodi, W., Zhang, L., & Müller, M. (2024). Characterization of structural and cytological markers across the cyclic phases of the female mammalian estrous cycle. *Biology of Reproduction*, 110(1), 78–89.
[27]. Yoest, K. E., Cummings, J. A., & Becker, J. B. (2019). Estrus cycle regulation of neuroendocrine and behavioral receptivity in female rodents. *Frontiers in Neuroendocrinology*, 53, 100–112.